

Using synchronous fluorescence spectroscopy and principal components analysis to monitor dissolved organic matter dynamics in a glacier system

J. D. Barker,^{1*} M. J. Sharp² and R. J. Turner³

¹ Department of Biological Sciences, University of Alberta, Edmonton, AB, T6G 2E9, Canada

² Department of Earth and Atmospheric Sciences, University of Alberta, Edmonton, AB, T6G 2E9, Canada

³ Department of Biological Sciences, University of Calgary, Calgary, AB, T2N 1N4, Canada

Abstract:

The molecular characteristics of dissolved organic matter (DOM) reflect both its source material and its biogeochemical history. In glacial systems, DOM characteristics might be expected to change over the course of a melt season as changes in the glacier drainage system cause the mobilization of DOM from different OM pools. To test this hypothesis we used Principal Components Analysis (PCA) of synchronous fluorescence spectra to detect and describe changes in the DOM in meltwater from a glacier system in the Coast Mountains of northern British Columbia, Canada. For most of the melt season, the dominant component of subglacially routed meltwater DOM is characterized by a tyrosine-like fluorophore. This DOM component is most likely derived from supraglacial snowmelt. During periods of high discharge, a second component of DOM is present which is humic in character and similar to DOM sampled from a nearby non-glacial stream. This DOM component is inferred to be derived from a moss-covered soil environment that has been glacially overrun. It is probably entrained into glacial melt waters when the supraglacial meltwater flux exceeds the capacity of the principal subglacial drainage channels and water floods areas of the glacier bed that are normally isolated from the subglacial drainage system. Another source of DOM also appears to be mobilized during periods of high air temperatures. It is characterized by both humic and proteinaceous fluorophores and may be derived from the drainage of supraglacial cryoconite holes. Copyright © 2009 John Wiley & Sons, Ltd.

KEY WORDS Principal Components Analysis; dissolved organic matter; synchronous fluorescence; Outre Glacier

Received 1 March 2007; Accepted 5 January 2009

INTRODUCTION

Dissolved organic matter (DOM) is a complex mixture of compounds of varying molecular weight and reactivity which plays a central role in the biogeochemistry and bioavailability of metals (e.g. Cabaniss, 1992; Thacker *et al.*, 2005), affects water column optical properties (e.g. Kowalczyk *et al.*, 2005), and is a potential nutrient source for microbial communities in aquatic environments (e.g. Coffin, 1989; Baker and Inverarity, 2004). The ecological function of DOM depends on its molecular composition and characteristics (e.g. aromatic versus aliphatic), which depend on its organic source material and biogeochemical history. In most freshwater and coastal aquatic environments, the primary source of DOM is plant matter (Stedmon *et al.*, 2003) and its degradation by biotic and abiotic processes during transport determines its ultimate molecular characteristics and ecological function.

In glacier systems, organic matter (OM) sources include OM in soils and vegetation that have been overrun during periods of glacier advance, and supraglacially-derived OM which is derived from OM in wind-deposited

sediment and algal production in the supraglacial (on top of the glacier) snowpack and/or cryoconite holes in ice at the glacier surface (e.g. Mueller *et al.*, 2001; Porazinska *et al.*, 2004). This supraglacially-derived OM may be transported to the glacier bed by meltwater draining vertically via moulins and crevasses, and can supplement the subglacial (beneath the glacier) OM pool. The subglacial environment is largely inaccessible to direct observation, and specific DOM sources and evidence of the biogeochemical processes that alter DOM are not readily determined. However, because the molecular characteristics of DOM reflect both OM source and biogeochemistry, the characteristics of DOM in meltwater issuing from beneath glaciers may provide an indication of OM sources and biogeochemical processes in both supraglacial and subglacial environments.

The compositional complexity of DOM imposes challenges for DOM characterization. Several analytical techniques focus on characterizing specific components of DOM (e.g. fulvic acid) even though the target component may represent only a small portion of the bulk DOM (e.g. McKnight *et al.*, 1991). As a result, the remainder of the bulk DOM remains uncharacterized. Fluorescence spectroscopy has emerged as a useful technique for characterizing the fluorescence properties, and thus the molecular

* Correspondence to: J. D. Barker, Department of Biological Sciences, University of Alberta, Edmonton, AB, T6G 2E9, Canada.
E-mail: jdbarker@ualberta.ca

characteristics, of bulk aquatic DOM (e.g. Coble, 2007; Hudson *et al.*, 2007). Fluorescence techniques provide information on the chemical characteristics of bulk DOM as a function of its component fluorescing functional groups (fluorophores). Fluorophores exist as a broad range of chemical compounds that comprise DOM (e.g. aromatic amino acids, humic material) which makes fluorescence spectroscopy well suited for bulk DOM characterization. Specifically, synchronous fluorescence spectroscopy rapidly provides high-resolution identification of DOM in bulk solutions containing multiple fluorophores by identifying them as individual peaks in the fluorescence spectrum while minimizing the spectral overlap between individual fluorophores (Ferrari and Mingazzini, 1995; Peuravuori *et al.*, 2002).

The complexity of a multi-peaked synchronous fluorescence spectrum makes the detection of subtle changes in spectral waveform from a large collection of spectra difficult. Statistical methods such as Principal Components Analysis (PCA) have been used to decompose complex multivariate signals into linearly independent components that characterize the variance in a given system (e.g. Hannah *et al.*, 2000; Bernat *et al.*, 2005).

The purpose of this investigation is to use PCA to characterize the variance in a collection of synchronous fluorescence spectra of DOM in glacier meltwater samples that were collected over the course of a melt season from a single glacier system and its surrounding aquatic environments. The goal of this analysis is to (a) identify DOM components and DOM sources; (b) detect temporal changes in DOM components; and (c) use this information to identify changes in either DOM source, or the extent and characteristics of biogeochemical alteration of a DOM source, in a glacial environment. DOM source and composition in glacier meltwater would be expected to change over the course of a melt season as the glacial drainage system evolves in response to changes in surface meltwater input (e.g. Nienow *et al.*, 1998). As the glacier drainage system changes, so too do the characteristics of potential supraglacial and subglacial DOM. Furthermore, there may be changes in the amounts of dissolved gases (O₂ and CO₂) in the meltwater that is delivered to the subglacial environment, that will influence the range of biogeochemical processes occurring subglacially (Tranter *et al.*, 2005).

FIELD SITE AND METHODOLOGY

Field site: Outre Glacier

Outre Glacier (56°14'N, 130°01'W) is a warm-based valley glacier (liquid water at the bed throughout the year) located in the Coast Mountains of northwest British Columbia, Canada (Figure 1). Outre Glacier currently terminates below the tree line (Figure 2a) in a coastal-temperate rainforest and it likely overran rainforest soils and vegetation during its Little Ice Age (LIA) advance. It may therefore have a subglacial pool of over-run rainforest-derived OM. Relict subglacial meltwater

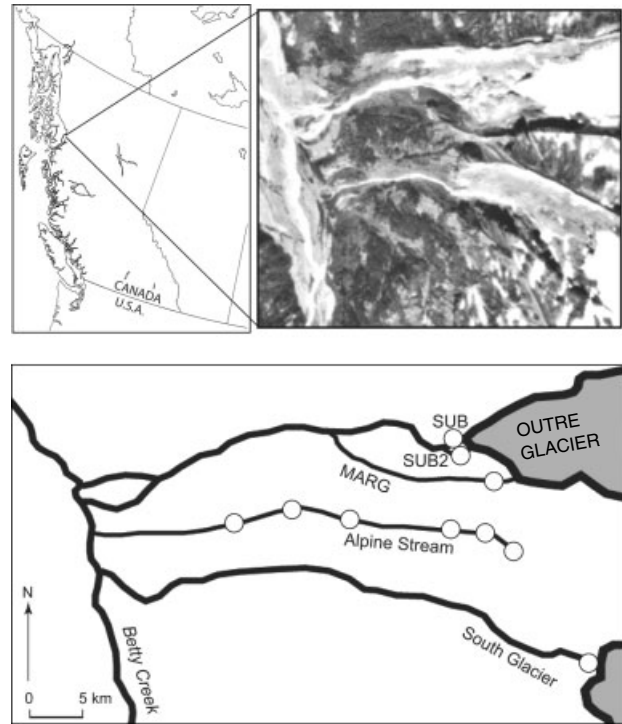


Figure 1. Location of the Outre Glacier field site. Open circles indicate sampling areas

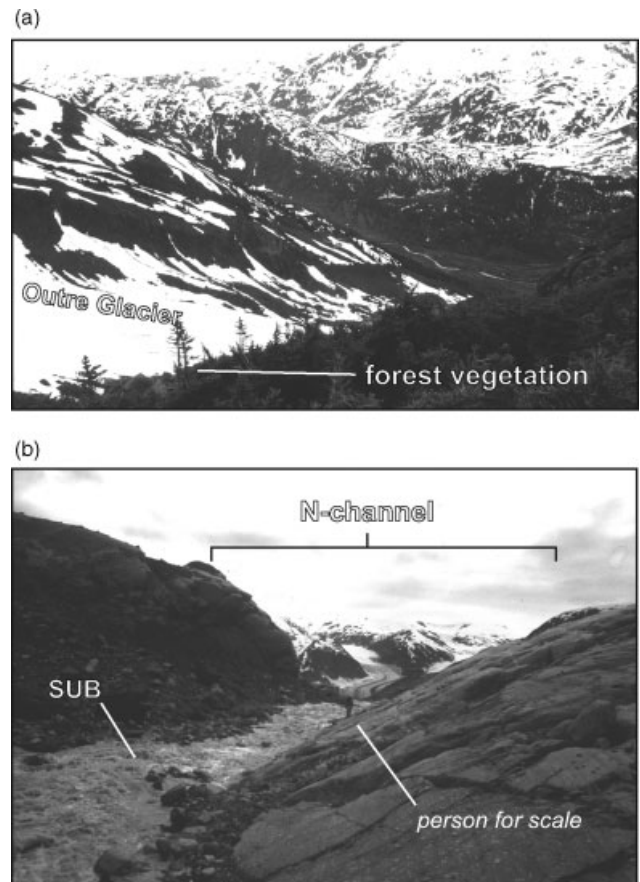


Figure 2. Photographs showing that (a) Outre Glacier terminates below, and is surrounded by forest vegetation; (b) the main subglacial meltwater stream (SUB) is confined by an incised bedrock channel (N-channel) at the Outre Glacier terminus

drainage channels are incised into sedimentary bedrock (N-channels) within the glacier forefield, and the main subglacial meltwater stream (SUB) that emerges from beneath the glacier is confined within an N-channel (Figure 2b).

Meltwater also drains from a second subglacial outlet (SUB2) later in the melt season, which is located at a slightly higher elevation (1161 m a.s.l.) than SUB (1153 m a.s.l.). SUB2 occupies a channel cut into the unconsolidated till (<0.3 m) which is draped over underlying bedrock.

The surface of Outre Glacier is heavily crevassed and supraglacial drainage (SUPRA) is routed via several small streams that flow for only short distances before descending into moulins and crevasses.

Outre Glacier also has a small marginal stream (MARG) that flows parallel to SUB, but is separated from it by a small drainage divide. MARG is supplied by supraglacial meltwater from the lower ablation zone that cascades off the glacier directly onto the proglacial bedrock surface. Discharge in MARG was very sensitive to changes in air temperature, which suggests that this stream is fed primarily by supraglacial melt from the lower ablation zone with no input from subglacial sources and minimal input from seepage from surrounding areas.

A small alpine stream (Alpine Stream) drains a non-glacierized catchment to the south of Outre Glacier (Figure 1). This stream originates as seepage from a moss-dominated alpine meadow and its discharge increases with distance towards the Betty Creek valley floor.

An unnamed warm-based valley glacier (referred to here as South Glacier) is located to the south of Alpine Stream (Figure 1). South Glacier currently terminates above the tree line, but a well-defined trimline further down valley indicates that it overran temperate rainforest soils and vegetation during its LIA advance. In contrast to Outre Glacier, the high terminal position of South Glacier suggests that a significant pool of overrun OM is unlikely to exist beneath this glacier. The inclusion of the South Glacier sampling site permits a comparison between a glacier lacking a significant subglacial OM pool (South Glacier) with one with a potentially significant subglacial OM pool (Outre Glacier).

Sampling

Meltwater from SUB and MARG was sampled at the approximate times of daily minimum and maximum discharge during July and August, 2002. SUB2 was also sampled after flow from this source was initiated on August 13. SUPRA meltwater was sampled from small supraglacial streams immediately below the snowline twice during the melt season, on July 18 and 19. The Alpine Stream and South Glacier subglacial stream were sampled opportunistically. On July 29, a series of samples was collected along the course of the Alpine Stream in order to sample DOM from different rainforest environments, as defined by differences in the dominant vegetation surrounding the stream (e.g. moss (*Lycopodium*

spp.), Sitka willow (*Salix sitchensis*), Sitka alder (*Alnus sinuata*) and Amabilis fir (*Abies amabilis*)).

All water samples were collected in 250 ml amber glass bottles. Each bottle was rinsed three times with sample water before the analytical sample was collected. DOM is commonly defined as that OM which passes through a glass fibre filter (GF/F; 0.7 μm) (e.g. De Souza Sierra *et al.*, 1994; Stedmon *et al.*, 2003; Yamashita and Tanoue, 2003). Samples were filtered onsite using a glass filtration apparatus that had been rinsed with 2N HCl and deionized water and fitted with a pre-combusted GF/F filter paper. The sample chamber was rinsed three times with sample water before 150 ml was decanted for filtration. The filtrate chamber was rinsed three times with filtrate before the remainder of the sample was filtered. The filtrate was then decanted in duplicate into acid washed and pre-combusted 40 ml amber glass vials. Filtered water samples were stored in the dark and kept cool ($\sim 5^\circ\text{C}$) until transport to the University of Alberta for analysis at the end of the field season.

Meltwater at the end of the field season was sampled in duplicate. One of the duplicate samples was analysed with all of the other fluorescence samples while the other sample was stored and analysed after ~ 3 months (the time evolved from the stream sampling at the beginning of the field season until spectroscopic analysis) to determine the effect of sampling storage on DOM characteristics. The results of the fluorescence analysis of the duplicate samples (not shown) indicate that sample storage did not affect DOM characteristics.

Debris-rich basal ice (BASAL) was sampled from locations along the north margin of the Outre Glacier terminus where glacier flow had created cavities on the lee side of bedrock obstacles. All of the equipment used for basal ice sampling was ethanol washed and flame sterilized. Prior to sampling, the basal ice face was cleaned by removing the first 10 cm of ice from the surface. Basal ice was chipped away with a chisel and collected in an aluminium tray and transferred into sterile Whirlpak bags. Laboratory experimentation indicates that sample storage in Whirlpak bags does not introduce fluorescing compounds to the sample. The basal ice was left to melt in a dark container in the laboratory at ambient temperatures, filtered and stored as described for the water samples (above).

Fluorescence analysis

After transport to the laboratory, meltwater samples were stored in the dark at 4°C until analysis (1 month after arrival at the University of Alberta). Synchronous fluorescence spectra were obtained using a SPEX Fluorolog-3 spectrofluorometer. The fluorometer was equipped with both excitation and emission monochromators with a Xenon lamp as an excitation source. Scans were performed on samples that had warmed to room temperature (21°C) at 1 nm increments with a 0.1 s integration period using a 10 nm bandwidth and an 18 nm offset ($\Delta\lambda = 18$ nm) between monochromators.

Water samples were contained within a quartz glass cuvette with a 10 nm pathlength. All spectra were Raman corrected by subtracting the synchronous spectrum of deionized water derived under identical scanning conditions. All scans were dark corrected and internally corrected to compensate for variations in lamp performance. The shapes of synchronous spectra are a function of $\Delta\lambda$. Multiple synchronous scans were performed on several meltwater samples using different offsets and a $\Delta\lambda$ of 18 nm was found to provide the best resolution of the multiple fluorophores that were present in the samples (data not shown).

Other studies (e.g. Miano and Senesi, 1992; Peuravuori *et al.*, 2002) also found that $\Delta\lambda = 18$ nm is optimal for samples which contain multiple fluorophores, such as are found in fulvic and humic acid samples. Studies that use a different $\Delta\lambda$ will report a different spectral peak wavelength for identical fluorophores, and the magnitude of this difference will be proportional to the difference in $\Delta\lambda$ used. Because of this, care must be taken when comparing spectral peak wavelengths from different studies. However, even although peak positions may change, studies using similar $\Delta\lambda$ will report peak wavelengths within a region, and this region can be used to compare spectral peaks between studies.

Similarly, fluorophore spectral peak locations derived using different fluorescence spectroscopic techniques may occur within a similar range. For example, the emission wavelength for spectral peak locations cited for fluorophores identified using the total luminescence technique, from which excitation-emission matrices (EEMs) can be derived, can potentially be used to define a region on the synchronous fluorescence spectrum where similar fluorophores would be expected to be found, especially when relatively low $\Delta\lambda$ are used (e.g. Sierra *et al.*, 2005). All of the synchronous spectra obtained in this study were smoothed using a centred 4 point discrete average with a 1 point overlap and normalized to the highest peak within each individual spectrum to ensure that the PCA focused on identifying variations in spectral shape (fluorophore composition) rather than spectral intensity. Fluorophore identification was based on comparisons with results reported in the literature (Table I).

Principal components analysis (PCA)

PCA was performed using STATISTICA v.5 (StatSoft) statistical software. PCA is used to identify principal components (PCs) that can be interpreted as 'type' spectra that permit the identification of compounds which comprise, and account for the bulk of the variation in, the fluorescence spectra of DOM derived from the Outre Glacier region. The potential non-independence of the spectral data collected here, which is common in time series datasets and which may invalidate the use of PCA where the goal is inferential in nature, should not affect the descriptive nature of the analysis presented here (Jolliffe, 1986).

Several PCAs were conducted on the fluorescence spectra from Outre Glacier and surrounding environments. The first PCA included all of the fluorescence spectra collected during the field season (referred to as TOTAL). A data matrix was constructed where spectra from each sample were arranged chronologically as variables (x axis) within each glacier environment that was sampled (SUB, SUB2, MARG, Alpine Stream, South Glacier, BASAL, SUPRA). The y axis consisted of the normalized fluorescence that is associated with a given wavelength. The input matrix consisted of 137 variables (spectra) and 101 cases (wavelengths). PCAs were also conducted for individual environments. The spectra for individual environments were arranged in chronological order as outlined above for the TOTAL PCA. All matrices were rotated using the *Varimax Raw* algorithm (when more than one PC was retained) to maximize the variance between spectra (columns) and maximize the loading on individual PCs in the data matrix (StatSoft, 1995).

The data matrix was ill-conditioned for all of the PCAs. Ill-conditioning is the result of a high degree of inter-correlation among the variables. This is not unexpected with the dataset being analysed here as minor changes in DOM source and biogeochemical history will result in subtle changes in spectral waveform over the time series from a single environment, and would be expected to result in a high degree of correlation. To correct for this, and to permit the PCA, STATISTICA artificially reduces the degree of inter-correlation between variables by adding a small constant to the diagonal of the data matrix. The PC factor patterns are not affected by this procedure, but the estimates of the percentage of variance in the dataset accounted for by each PC will not be exact (StatSoft, 1995). However, the relative magnitudes of the percentage of variance explained by each PC should be retained.

RESULTS

The average synchronous fluorescence spectrum for the DOM in all 137 water samples indicates that the DOM is composed of 4 main fluorophores with several poorly resolved fluorophores at longer wavelengths (Figure 3). The standard deviations associated with each spectral peak suggest that the relative contribution of each fluorophore to the bulk fluorescence varies between samples and that the magnitude of the standard deviation varies between fluorophores over the time series. The presence of a shoulder on the 420 nm peak and the asymmetry of the 365 nm peak suggest that additional fluorophores may be present but that they are ill-defined in the average spectrum plot. PCA is used here to help resolve these complexities.

TOTAL PCA

The PCA of all 137 synchronous spectra (TOTAL PCA) yielded 2 PCs that account for 95% of the variance (Figure 4). The plots of PCA factor scores (values for

Table I. Fluorescence peak designation

compound (scan parameter)	peak wavelength (nm)	source
phenylalanine standard (EEM)	255–265	Yamashika and Tanoue, 2003
phenylalanine ($\Delta\lambda = 10$ nm)	263	Sikorska <i>et al.</i> , 2004
tyrosine-like (EEM)	265–280	Yamashika and Tanoue, 2003
tyrosine standard (EEM)	270–275	Yamashika and Tanoue, 2003
monoaromatics ($\Delta\lambda = 25$ nm)	270–300	Ferrari and Mingazzini, 1995
protein- and/or phenol-like ($\Delta\lambda = 20$ nm)	275	Sierra <i>et al.</i> , 2005
aromatic amino acids ($\Delta\lambda = 18$ nm)	280	Peuravuori <i>et al.</i> , 2002
tyrosine ($\Delta\lambda = 10$ nm)	283	Sikorska <i>et al.</i> , 2004
tyrosine-like (EEM)	275	Coble, 1996
tryptophan-like (EEM)	275	Coble, 1996
tryptophan-like (EEM)	275–285	Yamashika and Tanoue, 2003
tyrosine ($\Delta\lambda = 25$ nm)	277	Ferrari and Mingazzini, 1995
tryptophan standard (EEM)	280	Yamashika and Tanoue, 2003
tryptophan ($\Delta\lambda = 10$ nm)	296	Sikorska <i>et al.</i> , 2004
tryptophan ($\Delta\lambda = 25$ nm)	291	Ferrari and Mingazzini, 1995
marine humic (EEM)	300–330	Yamashika and Tanoue, 2003
protein-like ($\Delta\lambda = 18$ nm)	307	Lombardi and Jardim, 1999
protein-like (tyrosine) (EEM)	309–321	Hudson <i>et al.</i> , 2007
2 condensed ring systems ($\Delta\lambda = 25$ nm)	310–370	Ferrari and Mingazzini, 1995
marine humic-like (EEM)	312	Coble, 1996
fulvic acid (soil extract) (EEM)	315	Yamashika and Tanoue, 2003
soil fulvic acid ($\Delta\lambda = 18$ nm)	317	Lombardi and Jardim, 1999
naphthalene ($\Delta\lambda = 18$ nm)	330	Peuravuori <i>et al.</i> , 2002
naphthalene (EEM)	340–370	Baker and Curry, 2004
protein-like (tryptophan) (EEM)	340–381	Hudson <i>et al.</i> , 2007
humic-like (EEM)	350	Coble, 1996
humic (EEM)	350–365	Yamashika and Tanoue, 2003
fulvic acid ($\Delta\lambda = 18$ nm)	357–457	Miano and Senesi, 1992
marine DOM ($\Delta\lambda = 18$ nm)	352	Lombardi and Jardim, 1999
polycyclic aromatics (4 benzene) ($\Delta\lambda = 18$ nm)	355	Peuravuori <i>et al.</i> , 2002
fulvic acid ($\Delta\lambda = 25$ nm)	370–400	Ferrari and Mingazzini, 1995
marine humic-like (EEM)	380–420	Hudson <i>et al.</i> , 2007
Suwannee River fulvic acid (standard) ($\Delta\lambda = 20$ nm)	400	Chen <i>et al.</i> , 2003
polycyclic aromatics (5 benzene) ($\Delta\lambda = 18$ nm)	400	Peuravuori <i>et al.</i> , 2002
humic-like (EEM)	400–500	Hudson <i>et al.</i> , 2007
fulvic acid ($\Delta\lambda = 18$ nm)	400–520	Miano <i>et al.</i> , 1988
humic acid ($\Delta\lambda = 18$ nm)	405–495	Miano and Senesi, 1992
polycyclic aromatics (7 benzene) ($\Delta\lambda = 18$ nm)	460	Peuravuori <i>et al.</i> , 2002
lignin descriptors ($\Delta\lambda = 18$ nm)	460	Peuravuori <i>et al.</i> , 2002
humic acid ($\Delta\lambda = 20$ nm)	470	Chen <i>et al.</i> , 2003
humic acid ($\Delta\lambda = 25$ nm)	470 and above	Ferrari and Mingazzini, 1995
humic acid ($\Delta\lambda = 18$ nm)	475–480	Miano <i>et al.</i> , 1988
humic acid standard ($\Delta\lambda = 25$ nm)	475	Ferrari and Mingazzini, 1995
soil fulvic acid ($\Delta\lambda = 18$ nm)	486	Lombardi and Jardim, 1999
phycoerithine (algal pigment) ($\Delta\lambda = 18$ nm)	566	Lombardi and Jardim, 1999

each case) versus wavelength provide an indication of the spectral waveform of each PC and therefore identify the fluorophores that contribute to the variance in the spectral signals. A comparison between the fluorophores detected here and those that have previously been characterized as specific compounds (Table I) permits a tentative identification of the fluorophores detected in this study.

TOTAL PC1 (91% of the variance) is associated with a single fluorophore at 273 nm (Figure 4), which is indicative of protein-like moiety in the DOM, specifically tyrosine (Tables I, II). TOTAL PC2 (4% of the variance) is associated with a primary fluorophore that is centred at 363 nm (Figure 4), which is indicative of humic material, specifically fulvic acid (Tables I, II). Humic material is a general term that is used to describe material formed by the abiotic condensation of reduced OM and includes

humic acid (water soluble at $\text{pH} > 2$), fulvic acid (water soluble at any pH) and humin (insoluble in water) (Sylvia *et al.*, 1999).

The loading of each spectrum on each PC provides an indication of how well each PC correlates with an individual synchronous fluorescence spectrum. Figure 5 shows that spectra from samples that load heavily on each PC are distinct. This demonstrates that the PCs capture features that are present in the fluorescence spectra and are not artefacts of the PCA.

The loadings of individual spectra on each TOTAL PC are displayed in Figure 6. Both TOTAL PCs show variance in loading over the course of the melt season and trends in PC loading can be discerned. Spectra from the lower reaches of the Alpine Stream load most heavily on TOTAL PC1 and BASAL spectra load most heavily on

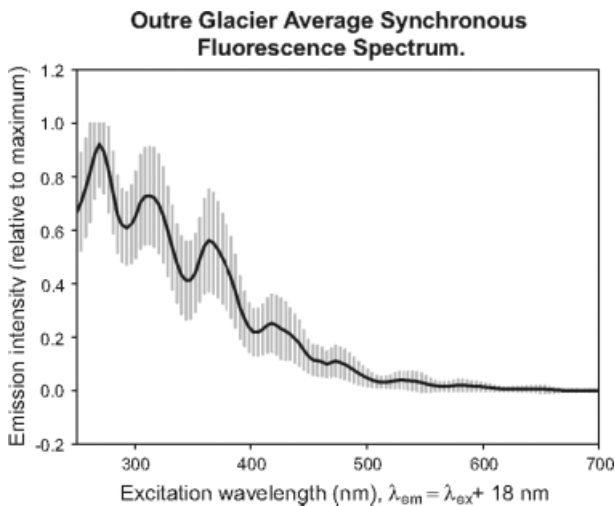


Figure 3. The average synchronous fluorescence spectrum from Outre Glacier (n = 116). The shaded area indicates one standard deviation from the mean

TOTAL PC2 (Figures 5, 6) suggesting that lower Alpine Stream DOM exhibits tyrosine-like fluorescence while basal ice (BASAL) spectra exhibit humic-like fluorescence. Furthermore, loading on TOTAL PC1 increases in subglacial meltwater until August 14 (day 226); whereafter loading on TOTAL PC1 decrease significantly (*t*-test, $P < 0.05$). Loading on TOTAL PC2 increase, after August 14 until the end of the monitoring period. This shift in spectral loading on August 14 coincides with the initiation of meltwater flow from SUB2. Spectra from SUB2 load similarly on TOTAL PCs 1 and 2. Of note is the sharp increase in TOTAL PC1 loading on August 13 (day 225; Figure 6). This increase in TOTAL PC1 loading is indicative of an increase in the tyrosine-like fluorophore (TOTAL PC1) in the bulk DOM spectral waveform (Figure 4, Table II). Loading on the spectra from South Glacier on TOTAL PCs 1 and 2 resembles that from SUB at the beginning of the monitoring period. This suggests that South Glacier DOM is similar to DOM in Outre Glacier subglacial meltwater early in the melt season.

Although TOTAL PC1 accounts for the majority of the variance (91%) in the spectra from all 137 samples, there

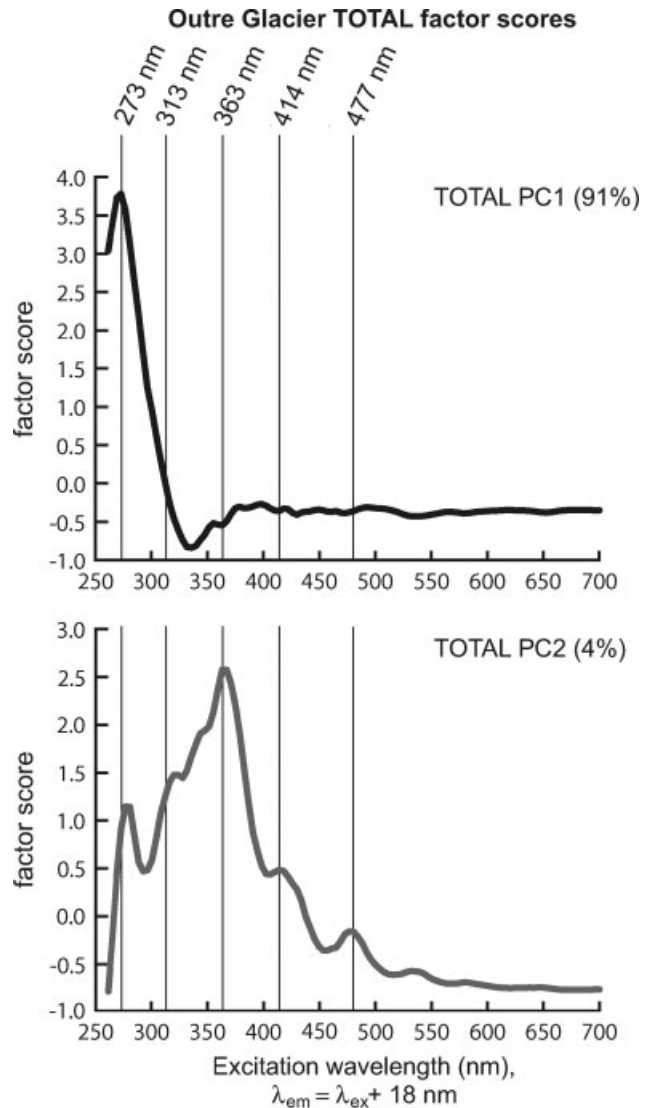


Figure 4. TOTAL PCA factor scores vs. spectral wavelength. These plots indicate which spectral shapes are associated with the variance in the overall signal, which is used to identify the fluorophores that contribute to the variance in the Outre Glacier DOM. The bracketed values indicate the percent of the overall variance that each PC represents

are some spectra that load more heavily on TOTAL PC2. For the purpose of comparison, the loadings for TOTAL

Table II. Principal component summary

Principal Component	Fluorophore	Dominant Fluorophore Identification
GROUP 1		
TOTAL PC1	273*	protein-like (tyrosine)
SUBGLACIAL PC1	268*, 304	protein-like (tyrosine)
MARG PC1	268*, 363	protein-like (tyrosine)
ALPINE STREAM	273*, 313, 363, 420, 477	protein-like (tyrosine)
SOUTH GLACIER	273*, 313, 363, 420, 477	protein-like (tyrosine)
GROUP 2		
TOTAL PC2	273, 322, 347, 365*, 414, 479, 531	humic-like
SUBGLACIAL PC2	273, 322, 365*, 414, 479, 534	humic-like
MARG PC2	237, 322*, 414, 477, 534	humic-like
BASAL	273, 322, 347, 365*, 420, 479, 534	humic-like

* indicates the dominant fluorophore.

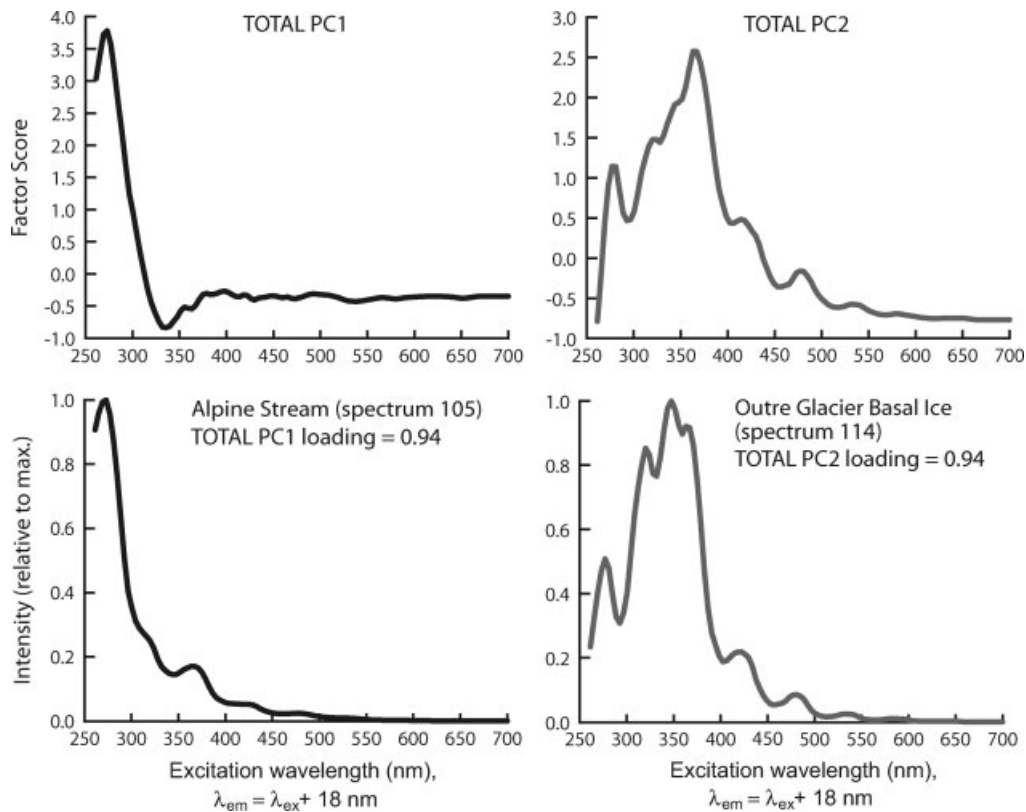


Figure 5. The relationship between the shape of each TOTAL PC and the shape of individual spectra that load strongly on them. Note that strong loadings indicate a similarity between spectral shapes of the TOTAL PCs and the individual spectra

PC1 are plotted against those for TOTAL PC2 (Figure 7). Although the spectrum which corresponds to the August 13 SUB sample (spectrum 34) does not fall outside 2 standard deviations of the mean, it is loaded the most strongly on TOTAL PC1 and most weakly on TOTAL PC2 of any of the SUB samples (Figure 6). This suggests that the SUB DOM has a predominantly tyrosine-like character on August 13. Other spectra that load most significantly on TOTAL PC1, relative to TOTAL PC2, are the spectra from the lower reaches of the Alpine Stream and from MARG on August 14 (Figure 7).

Similar to the decrease in SUB spectral loading on TOTAL PC1 on August 14, the MARG spectral loading on TOTAL PC1 decreases significantly (t -test, $P < 0.05$) to levels that are similar to TOTAL PC2 loading on August 15 (day 227, Figure 6) and persists until August 20 (day 232). This indicates that the DOM in supraglacial meltwater changed from predominantly tyrosine-like to more humic-like from August 15–20. While this is not the first time that TOTAL PC1 loading decreases in the supraglacial environment, it is the only time that this decrease persists for several days.

Spectra from supraglacial meltwater samples (MARG) load more heavily on TOTAL PC1 relative to TOTAL PC2 than do spectra from the subglacial environment for most of the melt season (Figure 6). This indicates that the supraglacial DOM is different than subglacial DOM. Thus, there will therefore be more variance in the spectral dataset when both supraglacial and subglacial fluorescence spectra are analysed together. Therefore,

a PCA of spectra from individual environments (e.g. subglacial, supraglacial) would be less influenced by variance due to the influence of spectra from other environments and might provide more information on the characteristics of specific pools of DOM within the study area.

Figure 8 depicts the PCs identified by a PCA of each environment at the Outre Glacier site. Note that the factor scores for SUB and SUB2 are perfectly correlated ($r^2 = 1$; Table III). Therefore, a single PCA was performed on spectra from SUB and SUB2 to characterize DOM from the subglacial environment (SUB-GLACIAL). For the sake of discussion, the PCs can be divided into two groups (Table II): Group 1 includes those PCs where the tyrosine-like fluorophore is the primary peak (SUBGLACIAL PC1, MARG PC1, Alpine Stream, South Glacier) and are more similar to TOTAL PC1. Group 2 includes those PCs that do not have the tyrosine-like fluorophore as the primary peak (SUB-GLACIAL PC2, MARG PC2, BASAL) and is more similar to TOTAL PC2.

Group 1: TOTAL PC1, SUBGLACIAL PC1, MARG PC1, Alpine Stream, South Glacier

Tyrosine biosynthesis occurs in both plants and microorganisms and is derived from chorismate, a product of the shikimate pathway (Schmid and Amrhein, 1999). Microbial tyrosine biosynthesis occurs in the cytoplasm where 90% of chorismate is used for amino acid synthesis whereas in plants it is believed to occur in the

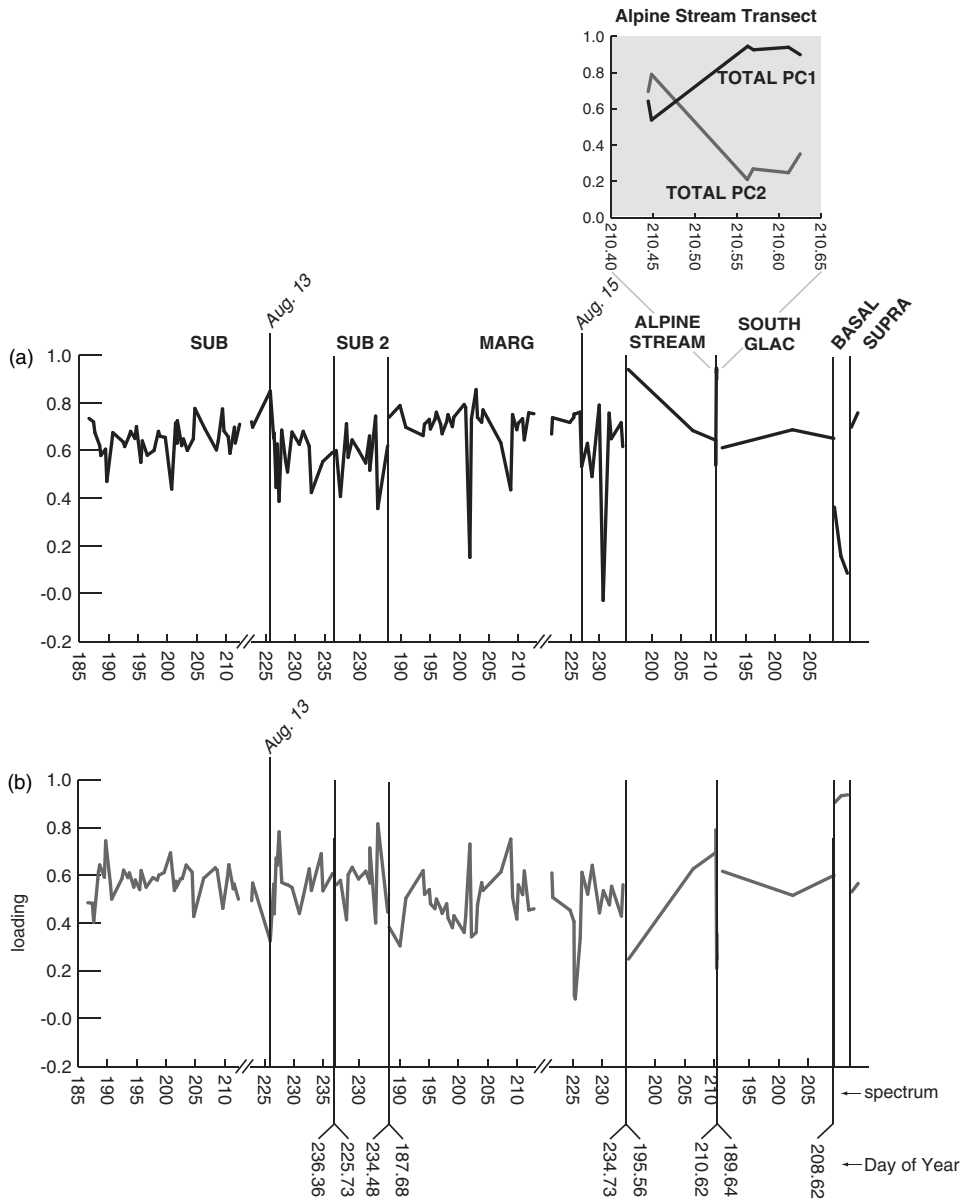


Figure 6. Factor loadings for (a) TOTAL PC1 and (b) TOTAL PC 2. The spectra are arranged chronologically within each environment

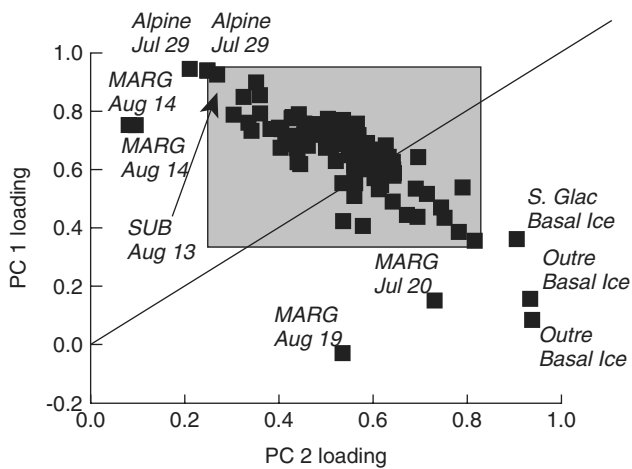


Figure 7. Synchronous spectra loading on TOTAL PC2 relative to TOTAL PC1. The grey box indicates two standard deviations from the mean on each loading

chloroplasts and is both less efficient than microbial tyrosine biosynthesis and produces secondary products such as lignin precursors and quinones (Schmid and Amrhein, 1999). Due to a tendency to transfer energy to other functional groups, tyrosine typically only fluoresces in the absence of associated tryptophan (Creighton, 1993) or humic substances (Yamashita and Tanoue, 2003). This suggests that the tyrosine detected in this study is indicative of either freshly produced amino acid that has not undergone molecular condensation and humification or bonded to existing humic material, or that there is insufficient humic material present to bind to all of the tyrosine in the meltwater. Furthermore, the existence of the prominent tyrosine fluorophore in TOTAL PC1, MARG PC1 and SUBGLACIAL PC1, and the absence of strong tryptophan, pigment or free quinone peaks suggest that the production of tyrosine is a product of a microbial metabolic pathway. These two lines of evidence suggest

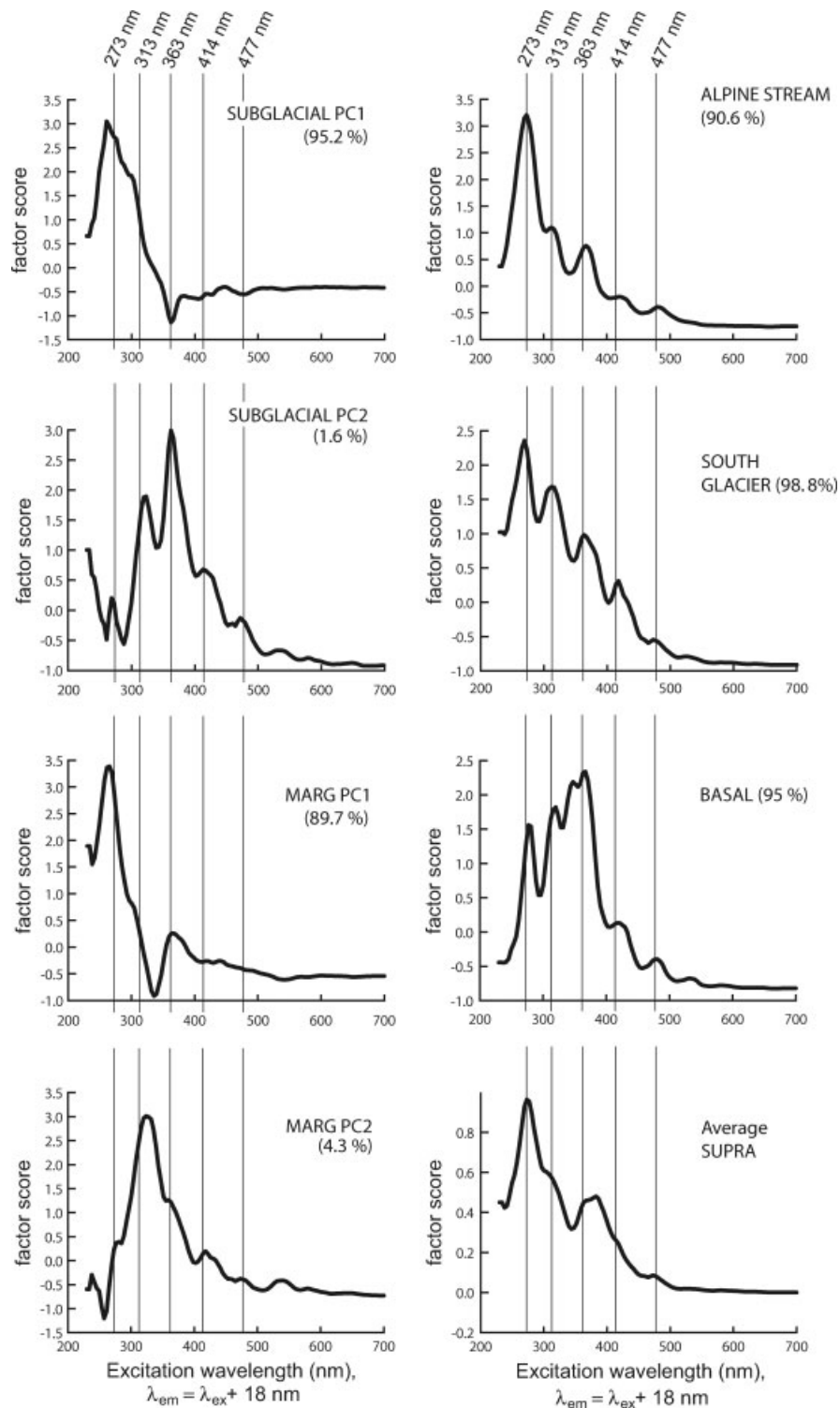


Figure 8. The spectral waveform for the PCs from each environment. The bracketed values indicate the percent of the variation that each PC represents. Note that the sample size for SUPRA was insufficient for PCA ($n = 2$) so the average spectrum is plotted here

that a microbial source is responsible for the observed tyrosine fluorescence.

A shoulder (304 nm) appears on the tyrosine peak in SUBGLACIAL PC1 (Figure 8). This coincides with the spectral range that is cited for protein-like fluorescence (Table I; Lombardi and Jardim, 1999). The presence of this fluorophore could result from either the presence of tryptophan or tyrosine metabolites (e.g. catechol) in the DOM (e.g. Determann *et al.*, 1998). The presence of the

tyrosine peak suggests the latter because tyrosine fluorescence is transferred to tryptophan if both amino acids are present (Yamashita and Tanoue, 2003). The expression of the tyrosine-like fluorophore suggests that such an energy transfer is not occurring and that tryptophan is not present.

A similar phenomenon is observed in MARG PC2 where the main aromatic amino acid peak (268 nm) is slightly blue-shifted relative to TOTAL PC1 (273 nm),

Table III. Correlation matrix for PC scores

	TOTAL PC1	TOTAL PC2	TOTAL PC3	TOTAL PC4	SUB SUB2	SUBGL- ACIAL PC1	SUBGL- ACIAL PC2	MARG PC1	MARG PC2	Alpine Stream	South Glacier	BASAL	
TOTAL PC1	1	0	0	0	0.65	0.60	0.92	-0.70	0.91	-0.06	0.86	0.65	0.20
TOTAL PC2		1	0	0	0.58	0.59	0.02	0.85	0.04	0.84	0.44	0.58	0.95
SUB				1	1	0.75	0.66	0.78	0.62	0.93	1	0.78	
SUB2					1	0.71	0.70	0.76	0.64	0.91	1	0.79	
SUBGLACIAL PC1						1	0	0.88	0.15	0.87	0.75	0.27	
SUBGLACIAL PC2							1	0.19	0.76	0.42	0.66	0.86	
MARG PC1								1	0	0.88	0.78	0.29	
MARG PC2									1	0.41	0.61	0.86	
Alpine Stream										1	0.93	0.65	
South Glacier											1	0.77	
BASAL												1	

but is still indicative of the presence of tyrosine (Tables I, III).

Group 2: TOTAL PC2, SUBGLACIAL PC2, MARG PC2, BASAL

The dominant peak in the TOTAL PC2, SUBGLACIAL PC2 and BASAL spectral waveforms is located at 365 nm with secondary peaks at 414 nm and 479 nm (Figures 4 and 8) and is indicative of the presence of humic material (Tables I, II). The two shoulders on the main humic material peak at 322 nm and 347 nm (TOTAL PC2 and BASAL) fall within the spectral range cited for fulvic acid (Table I). The fact that these two shoulders bracket the naphthalene spectral region (330 nm; Table I) suggests that the humic material indicated by these two shoulders is derived from a refractory, possibly ligneous, source of OM. A fluorophore at 322 nm forms the prominent peak in MARG PC2 and is indicative of humic material (Figure 8; Tables I, II).

The presence of multiple fluorophores suggests a multiple source contribution to the DOM represented by the Group 2 PCs. This is similar to the spectral waveform characteristic of soil humic material (e.g. Miano and Senesi, 1992). Soil humic material is a product of the abiotic molecular condensation of a wide range of organic compounds that are derived from the surrounding environment (Sylvia *et al.*, 1999). In the case of Group 2 PCs, a combination of both labile (amino acid) and recalcitrant (humic material) OM sources contribute to the PC waveform. Furthermore, the presence of both tyrosine and humic material fluorescence suggests that the amino acid is not closely associated with the humic material because complete energy transfer from tyrosine to humic material has not occurred. The presence of an amino acid that is not associated with humic material would be expected in a soil environment where both biotic and abiotic processes are occurring simultaneously and fresh amino acids are produced or where water with pre-existing amino acids is mixing with humic material but has not yet bonded.

In summary, TOTAL PC1, SUBGLACIAL PC1, MARG PC1 and the Alpine Stream PC are correlated

(Table III) and show a dominant fluorophore at 273 nm that is indicative of a protein-like fluorophore, likely tyrosine. The South Glacier and SUPRA average spectrum also have their dominant fluorophore at 273 nm (Figure 8, Table II). The existence of the prominent protein-like fluorophore and the absence of fluorophores which are indicative of tryptophan, pigment or quinone peaks suggest that the tyrosine which is detected in Group 1 PCs is derived from a microbial source which is found in the supraglacial environment. TOTAL PC2, SUBGLACIAL PC2, MARG PC2 and BASAL are correlated (Table III) and show dominant fluorophores at longer wavelengths which are indicative of humic material (Figure 8, Table II). Of note is the fluorophore that occurs at 322 nm, the spectral region which is cited for soil fulvic acid (317 nm) and naphthalene (330 nm; Table I). The presence of this fluorophore suggests that the humic material in the spectra which are associated with TOTAL PC2, SUBGLACIAL PC2, MARG PC2 and BASAL may be derived from a refractory soil-derived and/or vascular plant source.

INTERPRETATION

The PCA of synchronous fluorescence spectra from Outre Glacier and surrounding environments yields 2 PCs that pick out several distinct fluorophores and account for 95% of the overall variance in the original spectra dataset. The spectral shape of each PC permits the identification of spectral 'types' which, depending on the fluorophores present in each PC and the relative loading of each PC on individual spectra, provide useful information concerning DOM composition and the relative contributions of different DOM sources to the original fluorescence spectra.

The most significant PC (TOTAL PC1) accounts for 91% of the variance in the full set of 137 fluorescent spectra, as well as the majority of variance in each sub-environment (except for basal ice; Figure 8), and is associated with a fluorophore that is indicative of a fresh microbial source of protein-like (tyrosine) DOM (Table II). The tyrosine fluorophore also features strongly in the SUPRA average plot (Figure 8). A second PC (TOTAL PC2) is characterized by fluorophores that

correspond to humic material. It accounts for 4% of the variance in the full set of spectra but accounts for 95% of the variance in basal ice spectra (Figure 8).

In subglacial meltwater samples there is a decrease in TOTAL PC1 loading and a corresponding increase in TOTAL PC2 loading on August 14, the day that flow from SUB2 was initiated (Figure 6). The initiation of subglacial meltwater flow from SUB2 is indicative of a change in the subglacial hydraulic system. The coincident change in DOM characteristics with the change in subglacial hydrology suggests that there is a hydrological control on the molecular characteristics of DOM in subglacial meltwater.

Conceptual model of subglacial meltwater drainage

The subglacial drainage system is generally viewed as having channelized and distributed components (Hubbard and Nienow, 1997). A network of linked cavities that covers a large area of the bed typically characterizes the distributed system and basal meltwater flows more slowly through this system than through the major subglacial channels. The distributed system is more likely to sequester meltwater and material which is derived from basal ice melt and subglacial sediments while the main channels drain supraglacially-derived meltwater and material that are delivered to the glacier bed via moulins and crevasses. When the supraglacial meltwater flux to basal channels exceeds channel capacity, overflow from the main conduits to the distributed system occurs and supraglacially derived meltwater may mix with meltwater and material from the distributed drainage system. As the volume of water in the channelized system decreases, or the channel volume increases to accommodate an increase in water flux (for example channel enlargement by melting of the ice that forms the roof of N-channel), the hydraulic gradient reverses and flow from the distributed system to the channelized system occurs. As a result of this mixing between meltwater in the channelized and distributed drainage systems, DOM in the bulk subglacial meltwater would reflect characteristics of both supraglacially and subglacially derived OM.

Subglacial DOM

The initiation of meltwater discharge from SUB2 on August 14 suggests that the meltwater flux in the main subglacial channel has increased. An increase in water depth in the main proglacial channel (Figure 9a), which is associated with relatively high daily average air temperatures (Figure 9b) on August 14, supports this hypothesis and is indicative of increased meltwater flux from the subglacial drainage system.

During periods of relatively low supraglacial meltwater input to the channelized component of the drainage system, and prior to the initiation of flow from SUB2, supraglacially-derived DOM dominates the fluorescence spectrum of subglacial DOM. Increases in the loading of SUB spectra on TOTAL PC1 (e.g. August 13 (day 225); Figures 6 and 7) may be indicative of supraglacial

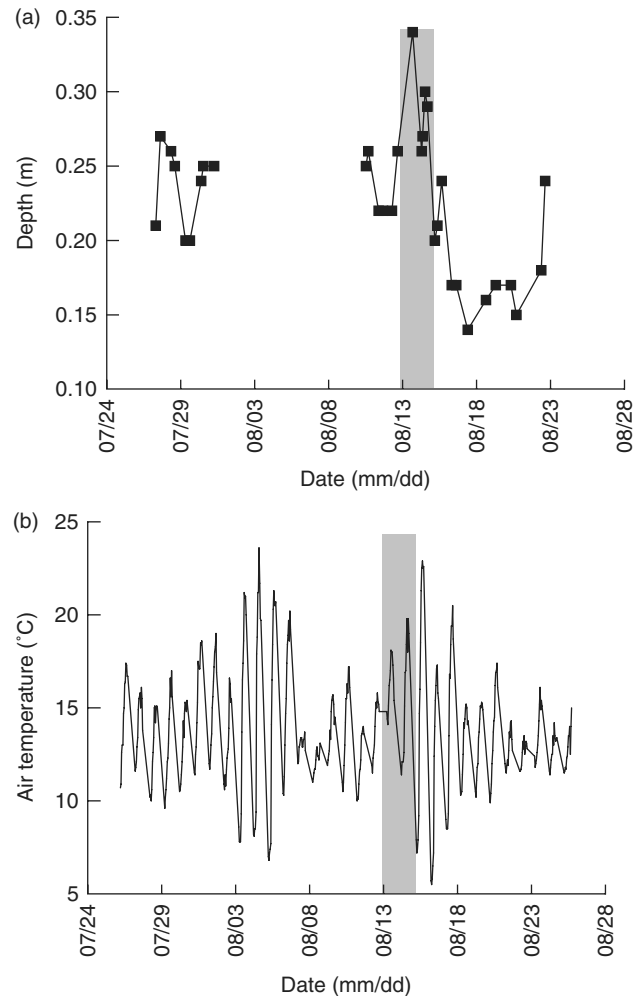


Figure 9. (a) the manually recorded water depth at a fixed point in the proglacial stream channel; (b) air temperature recorded at Stewart, B.C., which is located at sea level ~ 30 km from Outre Glacier. The shaded area indicates the period of time when the TOTAL PC loadings shift in the subglacial and marginal streams. Note that the shift corresponds to a period of high daily minimum temperatures

flushing due to relatively high daily average air temperatures. The fact that the protein-like fluorophore is associated with tyrosine (Tables I, II) and is prominent in the supraglacial spectra (SUPRA and MARG PC1) supports the hypothesis that the protein-like fluorophore may be derived from tyrosine production in supraglacial snow and ice melt.

During periods of relatively high supraglacial meltwater input, the hydraulic gradient from the channelized system to the distributed system creates a hydraulic connection between the two systems, as indicated by flow from SUB2 on August 14 (Figure 6). During periods of decreasing subglacial meltwater discharge, when the hydraulic gradient is from the distributed system to the channelized system, DOM derived from a humic source (as expressed most strongly in BASAL spectra; Figure 6) becomes a more prominent contributor to the subglacial DOM spectra. TOTAL PC1 loadings in SUB were significantly lower after August 14, indicating that the molecular characteristics of the subglacial DOM were different than they were earlier in the season.

The similarity between TOTAL PC1 and TOTAL PC2 loadings in SUB and SUB2 after August 14 (Figure 6a) suggests that a hydraulic connection has been established between the channelized and distributed drainage systems where supraglacially derived meltwater (containing protein-like DOM) is able to mix with meltwater from the distributed system (containing humic-like DOM), producing bulk subglacial meltwater which contains both types of DOM.

Just as discharge in the proglacial stream on August 14 was relatively high and corresponded to a relatively high daily minimum temperature, stream discharge was lower after August 14 and corresponded to relatively low minimum temperatures (Figure 9a, b). This suggests that after August 14, the hydraulic pressure in the channelized system was low thus promoting flow from the distributed system to the channelized system. The DOM that is represented by TOTAL PC2 has a similar fluorescence spectrum to SUBGLACIAL PC2 (Figure 8) and they are highly loaded on the BASAL spectra (Figures 6 and 7). They reflect a humic source of OM (Table II) and are most similar to the PC of streamflow from a moss-covered alpine meadow, as indicated by relatively high TOTAL PC2 loadings on upper Alpine Stream spectra (103 and 104; Figure 6). Again, the change in hydraulic pressure in the channelized system permitted the mixing of humic-like DOM from the distributed system with protein-like DOM in the bulk subglacial meltwater.

Spectra from subglacial meltwater at South Glacier resembles that found in Outre Glacier subglacial meltwater in the early melt season. This suggests that South Glacier does not have a significant pool of OM in the distributed component of its subglacial drainage system and/or its subglacial drainage system does not access a subglacial OM pool in the same manner that is observed at Outre Glacier. The fact that the terminus at South Glacier is located above the tree line supports the former hypothesis.

Supraglacial DOM

Hydrological conditions also govern the mobilization of DOM in the supraglacial environment. While the majority of the DOM that is mobilized supraglacially appears to be derived from a microbial source in the supraglacial snowpack, periods of exceptional melt may have stimulated the mobilization of OM from a secondary source, as represented by MARG PC2. Differences in the spectral waveform between MARG PC2 and SUBGLACIAL PC2 (Figure 8) suggest that the molecular characteristics of the secondary OM source are different between the two environments. For example, while both MARG PC2 and SUBGLACIAL PC2 have primary peaks that are indicative of humic material, those in MARG PC2 are indicative of a less condensed form of humic material than those in SUBGLACIAL PC2, as indicated by the shorter wavelength position of the primary peak. Additionally, the protein-like fluorophore is present as a well-defined peak in SUBGLACIAL PC2,

while it appears as a shoulder on the humic peak in MARG PC2.

In addition to these spectral shape differences, the timing of shifts in MARG spectral loadings on TOTAL PC1 and TOTAL PC2 also suggest that the source of this humic OM differed between the MARG and SUBGLACIAL environments. The sharp decrease in TOTAL PC1 loading occurred on August 15 (day 227) in MARG, a day later than it did in SUB (August 14). In SUB, this decrease in loading on TOTAL PC1 persisted until the end of the monitoring period due to the establishment of a hydrological connection between the subglacial channelized and distributed systems. The TOTAL PC2 increase in MARG persisted for only 5 days, until August 20 (day 232). These lines of evidence indicate that while the secondary source of OM in the subglacial environment may be overrun soil, most likely from a moss-covered environment, the secondary source of OM in MARG is different, although also derived from a soil-related environment.

A possible source of soil-related OM to the supraglacial environment is wind-blown sediment that has been deposited on the glacier surface and/or accumulated in cryoconite holes. Cryoconite holes are cylindrical depressions that result from the melting of dark wind-blown sediment into the glacier surface (Porazinska *et al.*, 2004). Microbial communities are known to exist in cryoconite holes (Porazinska *et al.*, 2004; Mueller *et al.*, 2001), so cryoconite OM may have both microbial and terrestrial characteristics, as is observed in the MARG PC2 spectral waveform. The event that stimulated the flux of microbially derived DOM from the supraglacial snowpack to the subglacial environment on August 13 (likely melt induced flushing) also stimulated a mobilization of a secondary source of OM in the lower ablation zone. It should be noted that air temperatures rose between August 12–15, after a relatively cooler period (August 7–11), and that minimum air temperatures were the highest recorded during the observation period (Figure 9b).

At Outre Glacier, most of the cryoconite holes are located higher in elevation (~1250 m a.s.l.) where the glacier surface slope is gentle enough to permit the accumulation of supraglacial sediment and the mobilization of the cryoconite DOM pool requires either a lowering of the glacier surface to below the cryoconite water level (e.g. Boon and Sharp, 2003) or supraglacial water flow through the cryoconite. The time lag between the subglacial change in OM properties in response to the melt event and the response in MARG may reflect the amount of time required to mobilize the DOM characterized by TOTAL PC2 and MARG PC2. Thus, the detection of cryoconite-derived DOM at the MARG sampling point would be delayed by either the supraglacial transit time required for meltwater to flow over the glacier surface and/or the time required to lower the glacier surface to allow cryoconite-derived meltwater to spill from the hole.

The small scale, high frequency (diurnal; Figure 6) variation in spectral loading on each PC that occurs throughout the subglacial and MARG records is likely the

result of hydrological variations in each environment. For example, changes in subglacial water pressure in response to supraglacial melt or precipitation input will control subglacial meltwater flow routing and DOM transport between the channelized and distributed drainage systems. Likewise, changes in supraglacial melt or precipitation will affect the mobilization of supraglacial DOM to MARG.

Non-glacial DOM

The spectra from the forested reaches of the Alpine Stream load most highly on TOTAL PC1 (mean = 0.94, Figure 6). This is an unexpected result because a higher proportion of fluorophores that are associated with vascular plant material (e.g. lignin biopolymers) or soils (e.g. humic material), which is represented by the fluorophores characteristic of TOTAL PC2, would be expected in the DOM from the mature forest reaches of the Alpine Stream because of its proximity to mature forest vegetation and developed soils. A possible explanation for this result is that the physically larger fraction of OM (POM (particulate organic matter), >0.7 μm) may be vascular plant derived while the finer fraction (DOM, <0.7 μm), which is considered here, may be derived from microbes in the water column (e.g. McKnight *et al.*, 1997). Spectra from the upper reaches of the Alpine Stream (waters draining from an alpine moss-covered soil environment) load heavily on TOTAL PC2, which suggests that vascular plant biopolymers and/or humic material are sufficiently small to be detected as DOM. This would be expected where vascular plant material is sparse and/or degraded into smaller biopolymers or where environmental conditions are conducive to the formation of humic material.

The upper Alpine Stream samples were taken from seepage flow that drains a moss covered meadow above the tree line in the non-glacierized catchment. This suggests that the soils in this area have high pore water content and that organic matter input to the soil environment is most likely derived from the moss cover rather than tree and/or root material. Wet conditions, in association with a largely non-ligneous plant OM input, favour the abiotic condensation of recalcitrant OM (non-microbial) to form humic material (Sylvia *et al.*, 1999).

SUMMARY AND CONCLUSIONS

PCA has been shown to be an effective technique for identifying the constituent components of synchronous fluorescence spectra of DOM from Outre Glacier. The DOM in water and basal ice at Outre Glacier and surrounding environments is composed of several fluorophores. These contribute to the bulk DOM fluorescence in different environments in varying degrees and at different times over the course of the melt season. PCA identifies 2 'type' fluorescence spectra (PCs), which account for 95% of the total variation in the spectral signal. The waveforms of each of these PCs indicate

that a protein-like (tyrosine) fluorophore, which may be derived from microbial biosynthesis in the supraglacial snowpack (TOTAL PC1), accounts for 91% of the variance in the overall spectral signal. This fluorophore also features prominently in the spectra from the Outre Glacier subglacial (SUBGLACIAL PC1), South Glacier subglacial (South Glacier PC), ice marginal (MARG PC1) and supraglacial (SUPRA) streams. The remaining PC displays a spectral waveform consisting of fluorophores which are indicative of a humic or a vascular plant/soil-derived source of DOM (TOTAL PC2). These fluorophores are also prominent in the lower order PCs from the individual environments (SUBGLACIAL PC2, MARG PC2) and in the basal ice spectra (BASAL PC).

Microbial DOM is flushed from the snowpack at Outre Glacier and transported through moulins and crevasses to the subglacial environment. This DOM dominates the DOM spectra in the supraglacial meltwater, but a second DOM pool which displays fluorophores which are indicative of humic material and may result from the drainage of supraglacial cryoconite holes, also contributes to the supraglacial DOM flux from August 15–20.

A second humic source of DOM is expressed more strongly in basal ice and in meltwater that has flowed through the distributed component of the subglacial drainage system. This suggests that a subglacial pool of DOM exists beneath Outre Glacier and may be derived from overrun moss-cover and underlying soil.

Hydrological flow conditions govern the mobilization of DOM in both the subglacial and supraglacial environment. An increased flux of supraglacial meltwater to the subglacial channelized system promotes meltwater flow, and thus a DOM flux, to the distributed system. A decrease in flow in the channelized system reverses the hydraulic gradient and promotes the flow of subglacial meltwater (and DOM) from the distributed system to the channelized system. A similar process has been described for subglacial dissolved solute transport (e.g. Tranter *et al.*, 1997).

While no clear indication of specific biogeochemical alteration to OM is evident from the analysis performed here, the presence of amino-acid fluorophores and humic fluorophores in the same PC (e.g. TOTAL PC2) suggests that the amino acids are recently produced and have not bound to humic material, which may be indicative of recent microbial biosynthesis.

Thus, the flux of DOM from Outre Glacier is dynamic. Given the strong influence of glacier hydrology to the characteristics of the net DOM flux, it may be possible to predict the characteristics of DOM exported from glacier systems given an understanding of both the characteristics of the various OM pools in the glacier system and characteristics of the specific glacier's seasonal hydrologic development.

ACKNOWLEDGEMENTS

We thank Ruth Bonneville for her valuable assistance at Outre Glacier. This research was supported by the Natural

Sciences and Engineering Research Council (NSERC) of Canada through a Discovery Grant to M.J. Sharp and Circumpolar/Boreal Alberta Research (C/BAR) and Northern Scientific Training Program (NSTP) grants to J.D. Barker. Insightful comments from two anonymous reviewers were helpful in improving this manuscript.

REFERENCES

- Baker A, Curry M. 2004. Fluorescence of leachates from three contrasting landfills. *Water Research* **38**: 2605–2613.
- Baker A, Inverarity R. 2004. Protein-like fluorescence intensity as a possible tool for determining river water quality. *Hydrological Processes* **18**: 2927–2945.
- Bernat E, Williams WJ, Gehring WJ. 2005. Decomposing ERP time-frequency energy using PCA. *Clinical Neurophysiology* **116**: 1314–1334.
- Boon S, Sharp MJ. 2003. Impact of an extreme melt event on the hydrology and runoff of a high Arctic glacier. *Hydrological Processes* **17**: 1051–1072.
- Cabaniss SE. 1992. Synchronous fluorescence spectra of metal-fulvic acid complexes. *Environmental Science and Technology* **26**: 1133–1139.
- Chen J, LeBoeuf EJ, Dai S, Gu B. 2003. Fluorescence spectroscopic studies of natural organic matter fractions. *Chemosphere* **50**: 639–647.
- Coble PG. 1996. Characterization of marine and terrestrial DOM in seawater using excitation-emission matrix spectroscopy. *Marine Chemistry* **51**: 325–346.
- Coble PG. 2007. Marine optical biogeochemistry: the chemistry of ocean color. *Chemical Reviews* **107**: 402–418.
- Coffin RB. 1989. Bacterial uptake of dissolved free and combined amino acids in estuarine waters. *Limnology and Oceanography* **34**: 531–542.
- Creighton TE. 1993. *Proteins: Structure and molecular properties*. W.H. Freeman: New York; 512.
- De Souza Sierra MM, Donard OFX, Lamotte M, Belin C, Ewald M. 1994. Fluorescence spectroscopy of coastal and marine waters. *Marine Chemistry* **47**: 127–144.
- Determann S, Lobbes JM, Reuter R, Rullkotter J. 1998. Ultraviolet fluorescence excitation and emission spectroscopy of marine algae and bacteria. *Marine Chemistry* **62**: 137–156.
- Ferrari GM, Mingazzini M. 1995. Synchronous fluorescence spectra of dissolved organic matter (DOM) of algal origin in marine coastal waters. *Marine Ecology Progress Series* **125**: 305–315.
- Hannah DM, Smith BPG, Gurnell AM, McGregor GR. 2000. An approach to hydrograph classification. *Hydrological Processes* **14**: 317–338.
- Hubbard B, Nienow P. 1997. Alpine subglacial hydrology. *Quaternary Science Reviews* **16**: 939–955.
- Hudson N, Baker A, Reynolds D. 2007. Fluorescence analysis of dissolved organic matter in natural, waste and polluted waters—a review. *River Research and Applications* **23**: 631–649.
- Jolliffe IT. 1986. *Principal Components Analysis*. Springer-Verlag: New York; 271.
- Kowalczyk P, Ston-Egiert J, Cooper WJ, Whitehead RF, Durako MJ. 2005. Characterization of chromophoric dissolved organic matter (CDOM) in the Baltic Sea by excitation emission matrix fluorescence spectroscopy. *Marine Chemistry* **96**: 273–292.
- Lombardi AT, Jardim WF. 1999. Fluorescence spectroscopy of high performance liquid chromatography fractionated marine and terrestrial organic material. *Water Research* **33**: 512–520.
- McKnight DM, Aiken GR, Smith RL. 1991. Aquatic fulvic acids in microbially based ecosystems: results from two desert lakes in Antarctica. *Limnology and Oceanography* **36**: 998–1006.
- McKnight DM, Harnish R, Wershaw RL, Baron JS, Schiff S. 1997. Chemical characteristics of particulate, colloidal, and dissolved organic material in Loch Vale Watershed, Rocky Mountain National Park. *Biogeochemistry* **36**: 99–124.
- Miano TM, Senesi N. 1992. Synchronous excitation fluorescence spectroscopy applied to soil humic substance chemistry. *The Science of the Total Environment* **117/118**: 41–51.
- Miano TM, Sposito G, Martin JP. 1988. Fluorescence spectroscopy of humic substances. *Soil Society of America Journal* **52**: 1016–1019.
- Mueller DR, Vincent WF, Pollard WH, Fritsen CH. 2001. Glacial cryoconite ecosystems: a bipolar comparison of algal communities and habitats. *Nova Hedwigia* **123**: 171–195.
- Nienow P, Sharp M, Willis I. 1998. Seasonal changes in the morphology of the subglacial drainage system, Haut Glacier d'Arolla, Switzerland. *Earth Surface Processes and Landforms* **23**: 825–843.
- Peuravuori J, Koivikko R, Pihlaja K. 2002. Characterization, differentiation and classification of aquatic humic matter separated with different sorbents: synchronous scanning fluorescence spectroscopy. *Water Research* **36**: 4552–4562.
- Porazinska DL, Fountain AG, Nylen TH, Tranter M, Virginia RA, Wall DH. 2004. The biodiversity and biogeochemistry of cryoconite holes from McMurdo Dry Valley glaciers, Antarctica. *Arctic, Antarctic and Alpine Research* **36**: 84–91.
- Schmid J, Amrhein N. 1999. The shikimate pathway. In *Plant Amino Acids: Biochemistry and Biotechnology*, Singh B.K. (ed). Marcel Dekker: New York; 147–169.
- Sierra MMD, Giovanela M, Parlanti E, Soriano-Sierra EJ. 2005. Fluorescence fingerprint of fulvic and humic acids from varied origins as viewed by single-scan and excitation/emission matrix techniques. *Chemosphere* **58**: 715–733.
- Sikorska E, Gorecki T, Khmelinskii IV, Sikorski M, De Keukeleire D. 2004. Fluorescence spectroscopy for characterization and differentiation of beers. *Journal of the Institute of Brewing* **110**: 267–275.
- StatSoft, Inc. 1995. *STATISTICA, Volume III, Statistics II*: 3201–3231.
- Stedmon CA, Markager S, Bro R. 2003. Tracing dissolved organic matter in aquatic environments using a new approach to fluorescence spectroscopy. *Marine Chemistry* **82**: 239–254.
- Sylvia DM, Fuhrmann JJ, Hartel PG, Zuberer DA. 1999. *Principles and applications of soil microbiology*. Prentice Hall: New Jersey; 550.
- Thacker SA, Tipping E, Baker A, Gondar D. 2005. Development and application of functional assays for freshwater dissolved organic matter. *Water Research* **39**: 4559–4573.
- Tranter M, Sharp MJ, Brown GH, Willis IC, Hubbard BP, Nielsen MK, Smart CC, Gordon S, Tulley M, Lamb HR. 1997. Variability in the chemical composition of in situ subglacial meltwaters. *Hydrological Processes* **11**: 59–77.
- Tranter M, Skidmore M, Wadham J. 2005. Hydrological controls on microbial communities in subglacial environments. *Hydrological Processes* **19**: 995–998.
- Yamashita Y, Tanoue E. 2003. Chemical characterization of protein-like fluorophores in DOM in relation to aromatic amino acids. *Marine Chemistry* **82**: 255–271.